Available online at www.sciencedirect.com
ScienceDirect
Polymer 49 (2008) 1145–1153
polymer
www.elsevier.com/locate/polymer

Coating of gold nanoparticles by thermosensitive poly(*N*-isopropylacrylamide) end-capped by biotin

Abdelhafid Aqil [a], Hongjin Qiu [a], Jean-François Greisch [b], Robert Jérôme [a], Edwin De Pauw [b], Christine Jérôme [a,*]

[a] *Centre for Education and Research on Macromolecules (CERM), University of Liège, Sart-Tilman, B6, 4000 Liege, Belgium*
[b] *Mass Spectrometry Laboratory, University of Liège, Sart-Tilman, B6, 4000 Liege, Belgium*

Received 19 July 2007; received in revised form 7 September 2007; accepted 8 December 2007
Available online 4 January 2008

Abstract

Gold nanoparticles (NPs) were prepared by reduction of $HAuCl_4$ in aqueous solution and stabilized by poly(*N*-isopropylacrylamide) (PNIPAM). PNIPAM was prepared by two distinct routes: (i) conventional free-radical polymerization leading to polymer without any reactive end-group, and (ii) Reversible Addition–Fragmentation chain Transfer (RAFT) polymerization with 2-dodecylsulfanylthiocarbonylsulfanyl-2-methyl propionic acid (DMP) as a RAFT agent. PNIPAM with low polydispersity was then end-capped by an α-carboxylic acid and an ω-trithiocarbonate that was converted into an ω-thiol upon hydrolysis. This hetero-telechelic polymer was analyzed by mass spectroscopy, size exclusion chromatography (SEC) and ^{1}H NMR. Even without thiol end-group, known for chemisorption onto gold, PNIPAM was effective in stabilizing gold NPs (~1–5 nm). The thermosensitivity of PNIPAM at the surface of gold NPs was, however, dependent on the molecular weight of the chains. Finally, the α-carboxyl end-group of PNIPAM was used to anchor biotin, which is indeed known for complexation with avidin, which is a possible strategy for the coated gold NPs to be involved as building blocks in supramolecular assemblies. TEM and UV–vis spectroscopy were used to characterize the gold nanoparticles.

Keyword: Hybrid materials; Nanoparticles; Thermoresponsive polymers

1. Introduction

The rapid growth of nanotechnology in the recent past is the direct consequence of the unique physical and chemical properties of nanoparticles (NPs) compared to bulk solids [1]. The intrinsic lack of stability of naked nanoparticles and their tendency to aggregate are highly undesirable, because of a deleterious impact on the optical, electrical, catalytic, and magnetic properties of the nanoparticles [2–4]. There is thus a need to build up a coalescence barrier (steric or else) around the nanoparticles [5]. There are many examples of stabilization of gold NPs by low molar mass alkylthiols. However, more recently, thiolated polymers were tested with success [6,7], particularly when they were prepared with pre-determined molecular characteristics by a living/controlled mechanism. In this respect, the Reversible Addition–Fragmentation Transfer (RAFT) polymerization is ideal, because the radical polymerization of many monomers can be controlled and the chains are end-capped by a trithiocarbonate or a dithioester group, which can be easily converted into thiol. In this case, a unique reagent is needed for the concomitant formation of the gold NPs and the stabilizer.

Another problem related to the NPs is their recovery after use, which is more acute when the stabilization is more effective. It is the reason why attention was paid to polymeric stabilizers, whose solvation is stimuli-dependent, such as poly(*N*-isopropylacrylamide) (PNIPAM), which is a water-soluble polymer with a lower critical solution temperature (LCST) in the 30–33 °C range [8–10]. The LCST behavior of PNIPAM

* Corresponding author. Tel.: +32 43663491; fax: +32 43663497.
E-mail address: c.jerome@ulg.ac.be (C. Jérôme).

0032-3861/$ - see front matter © 2007 Elsevier Ltd. All rights reserved.
doi:10.1016/j.polymer.2007.12.033

is commonly accounted by a balance between hydrogen bonding and the hydrophobic effect. PNIPAM has a hydrophilic amide group and a hydrophobic isopropyl group. Below the LCST, aqueous solutions are stabilized by hydrogen bonding between the amide groups and the water, and by ice-like structures that water molecules form around the hydrophobic groups. As the temperature is increased, the hydrogen bonding weakens and the attractions between hydrophobic groups increase leading to the eventual demixing of the PNIPAM chains above the LCST. Several applications take advantage of this temperature-sensitive water solubility, such as controlled drug delivery [11,12], separation [13] and catalysis [14].

First synthesized by Pelton's group [15], PNIPAM is commonly prepared by controlled radical polymerization, mainly by Atom Transfer Radical Polymerization (ATRP) [8,16,17] and RAFT [9,18,19,20]. Convertine et al. succeeded in analyzing PNIPAM by size exclusion chromatography (SEC) in DMF at 60 °C, thus under conditions that prevented parasitic polymer aggregation/adsorption from occurring [20]. The polydispersity index of PNIPAM prepared by RAFT was lower than 1.07. Tenhu et al. [19c] prepared PNIPAM by RAFT in the presence of 4-cyanopentanoic acid dithiobenzoate (CPADB), and they used this polymeric ligand to stabilize gold nanoclusters with a well controlled size and a reasonably narrow size distribution.

This work aims at preparing gold NPs protected/stabilized by biotinylated PNIPAM via a thiol anchoring end-group. The motivation for a biotin at the free chain-end of the stabilizer is the supramolecular assembly of the NPs by complexation with avidin in water. For this purpose, gold NPs were prepared in the presence of PNIPAM synthesized by RAFT with a carboxylic acid containing transfer agent. Biotin-cadaverine was finally attached to the gold NPs via the α-carboxyl end-group of the PNIPAM protective chains.

2. Experimental

2.1. Materials

N-Isopropylacrylamide (Aldrich, 97%) was twice recrystallized from a benzene/hexane mixture (3:2 v/v) and dried in vacuo prior to use. 4,4′-Azo-bis-(4-cyanopentanoic) acid (ACPA; Fluka, >98%) was used as received and 2,2′-azo-bis-(isobutyronitrile) (AIBN; Fluka) was recrystallized from methanol. *N*,*N*-Dicyclohexylcarbodiimide (DCC; Aldrich, 99%), hydrogen tetrachloroaurate(III) hydrate ($HAuCl_4 \cdot H_2O$; Strem, 99.9%), sodium hydroborate ($NaBH_4$; Janssen, 98%), *N*-hydroxysuccinimide (Aldrich, 97%), *N*-(5-aminopentyl)biotinamide (biotin-cadaverine) (Molecular probes), avidin (Aldrich), benzene (Lab Chemistry, 99%) and diethyl ether (Labotec, CP) were used as received. *N*,*N*-Dimethylformide (DMF; Aldrich, 99.9%) was dried over P_2O_5 prior to use. All the other solvents (the highest grade) were used as received.

2.2. Synthesis of 2-dodecylsulfanylthiocarbonylsulfanyl-2-methyl propionic acid (DMP): a RAFT chain transfer agent (CTA)

DMP was synthesized according to Lai et al. [21]. 1-Dodecanethiol (80.76 g, 0.4 mol), acetone (192.4 g, 3.31 mol), and aliquat 336 (tricaprylylmethylammonium chloride; 6.49 g, 0.016 mol) were mixed in a reactor cooled to 10 °C under nitrogen. A sodium hydroxide solution (50%) (33.54 g, 0.42 mol) was added over 20 min, and the reaction medium was stirred for additional 15 min before carbon disulfide (30.42 g, 0.4 mol) in acetone (40.36 g, 0.69 mol) was added over 20 min, which resulted in a red color. Ten minutes later, chloroform (71.25 g, 0.6 mol) was added, followed by the dropwise addition of the 50% sodium hydroxide solution (160 g, 2 mol) over 30 min, and the reaction mixture was stirred overnight; 600 mL of water were added, followed by 100 mL of concentrated HCl. Nitrogen was bubbled within the reaction medium under vigorous stirring in order to eliminate acetone. A solid product was filtered off with a Buchner funnel, then stirred in 1 L of isopropanol, filtered again and identified as *S*,*S*′-bis(1-dodecyl)trithiocarbonate. The isopropanol solution was concentrated to dryness, and the solid was recrystallized from hexane so yielding 92.5 g of a yellow crystalline solid. ^{1}H NMR (400 MHz, $CDCl_3$) 0.8 (t, 3H), 1.4 (m, 20H), 1.7 (s, 6H), 3.4 (t, 2H), 13 (s, 1H). Recrystallization was repeated until DMP was pure when analyzed by ^{1}H NMR.

2.3. Synthesis of PNIPAM–COOH by RAFT polymerization (CTA–PNIPAM–COOH)

PNIPAM with one carboxylic acid (–COOH) end-group was prepared by RAFT with DMP as a RAFT agent (Scheme 1), as reported elsewhere [20]. Briefly, in a previously flamed three-neck flask, recrystallized NIPAM (5.0 g), DMP (182 mg, 5×10^{-4} mol) and ACPA (9.24 mg, 2.5×10^{-5} mol) were dissolved in 20 mL of DMF. The solution was degassed by three freeze–thaw–evacuation cycles, and then the flask was transferred to a water bath at 25 °C. After 4 h, the crude reaction product was precipitated in diethyl ether. The procedure was twice repeated. The final slightly yellow powder was characterized by ^{1}H NMR (400 MHz, DMSO-d_6): 4.0 (1H, –N–CH<, s), 2.1 (1H, –C–CH– broad band), 1.65 (2H, $-CH_2-C-$ broad band), 1.20 (22H, $C_{11}H_{22}$), 1.13 (6H, CH_3-C-CH_3, broad band), and 0.8 (3H, $C-CH_3$). This PNIPAM sample was designated as CTA–PNIPAM–COOH.

2.4. Synthesis of PNIPAM by free-radical polymerization

PNIPAM was also synthesized by conventional free-radical polymerization. NIPAM (0.01 mol) and AIBN (0.35 mmol) were dissolved in DMF in a round-bottom flask kept in an ice bath. The solution was degassed by nitrogen for 30 min and heated in an oil bath at 70 °C for 3 h. PNIPAM was collected by precipitation in diethyl ether and dried. The molar mass was determined by SEC in DMF ($M_n = 110{,}000$, PDI = 1.95). This sample was designated as PNIPAM.

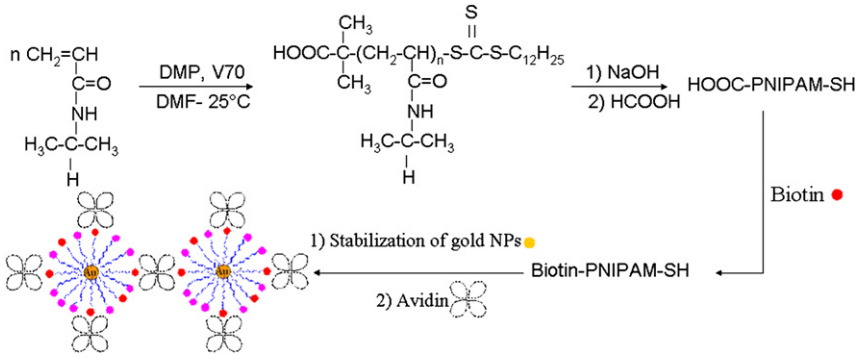

Scheme 1. Synthesis of α-carboxyl, ω-thiol PNIPAM by RAFT, and supramolecular assembly of biotin–PNIPAM–S–Au nanoparticles by tin–avidin complexation.

2.5. Hydrolysis of CTA–PNIPAM–COOH into HS–PNIPAM–COOH

CTA–PNIPAM was hydrolyzed by a NaOH solution in methanol (1.0 M, 28%) under nitrogen in the presence of a small amount of EDTA in order to prevent the in situ formed thiol from being oxidized. After hydrolysis, the mixture was acidified by 88% formic acid and ultrafiltrated through a 0.2 μm membrane (Nylon Acrodisc). After dialysis against deionized water for 3 days, the final product was recovered by lyophilization from water.

2.6. Biotinylation of SH–PNIPAM–COOH (HS–PNIPAM–biotin)

A mixture of HS–PNIPAM–COOH and DCC was dissolved in dried DMF. *N*-Hydroxysuccinimide dissolved in dried DMF was then added dropwise at 0 °C. The reaction medium was stirred at room temperature for 24 h, followed by the addition of *N*-(5-aminopentyl)biotinamide and triethylamine. The stirring was continued for additional 15 h. Dicyclohexylurea was eliminated by filtration through a 0.45 μm membrane. The unreacted biotin derivative was eliminated by dialysis against acidic water, and the solution was finally lyophilized.

2.7. Preparation of Au nanoparticles stabilized by HS–PNIPAM–COOH, and HS–PNIPAM–biotin

Gold nanoparticles were prepared according to McCormick et al. [22] except for the Au/S molar ratio that was 3.5:1 as recommended by Leff et al. [23]. In a typical experiment, PNIPAM (0.9×10^{-4} mol) and 10 mg of $HAuCl_4 \cdot 3H_2O$ were dissolved in 20 mL of deionized water, followed by the slow addition of 0.5 mL of a freshly prepared aqueous solution (0.45 M) of $NaBH_4$ ($NaBH_4/Au = 15.0:1$) under vigorous stirring. The reaction was kept under stirring for 12 h. The colloidal solution of HOOC–PNIPAM–S–Au (or biotin–PNIPAM–S–Au) was dialyzed against water for 3 days to remove the free PNIPAM chains and the excess of gold salt. Gold nanoparticles were collected by filtration through a 0.45 μm membrane prior to characterization. The colloidal solutions of gold nanoparticles were dark blue.

2.8. Characterization

2.8.1. Polymers

They were analyzed by ^{1}H NMR spectroscopy with a Bruker AM 400 apparatus at 25 °C, in deuterated chloroform ($CDCl_3$) added with tetramethylsilane as an internal reference. Number-average molecular weight was calculated from the intensity ratio of the CH protons of the NIPAM units ($\delta = 4.0$) and the CH_3 protons of DMP. The polydispersity index (PDI) was determined by size exclusion chromatography (SEC) with a 25 mM solution of LiBr in DMF as eluent at 50 °C. Polystyrene standards were used for calibration. MALDI-TOF mass spectrometry was carried out with a Bruker Reflex III equipped with a 337 nm N_2 laser in the reflector mode and a 20 kV acceleration voltage. Dithranol (Aldrich, 97%) was used as the matrix. Sodium or potassium trifluoroacetate was added for ion formation. Samples were prepared by mixing matrix (20 mg/mL), sample (10 mg/mL) and salt

Table 1
Molecular characteristics of PNIPAM used in this work

Process	Time (h)	Conversion[b] (%)	M_n				IP[e]	LCST[f] (±0.02 °C)
			Theoretical	Experimental[c]	MS[d]	SEC[e]		
RAFT[a]	3	30	3000	2500	2000	17,800	1.05	21.00
RAFT[a]	5	50	5000	4500	4000	62,000	1.05	32.22
Free	3	–	–	–	–	110,000	2.00	31.50

[a] Solvent, DMF; temperature, 25 °C; [NIPAM]/[DMP]/[V70] = 1767/20/1; [NIPAM] = 2.2 M.
[b] Determined from ^{1}H NMR spectrum of the reaction mixture in DMSO-d_6.
[c] Determined by NMR.
[d] Determined by MALDI-TOF MS.
[e] Determined by SEC using 25 mM solution of LiBr in DMF as the eluent at 50 °C, and calibration based on polystyrene standards.
[f] Determined by UV–vis spectroscopy (inflection point of the absorbance–temperature curve).

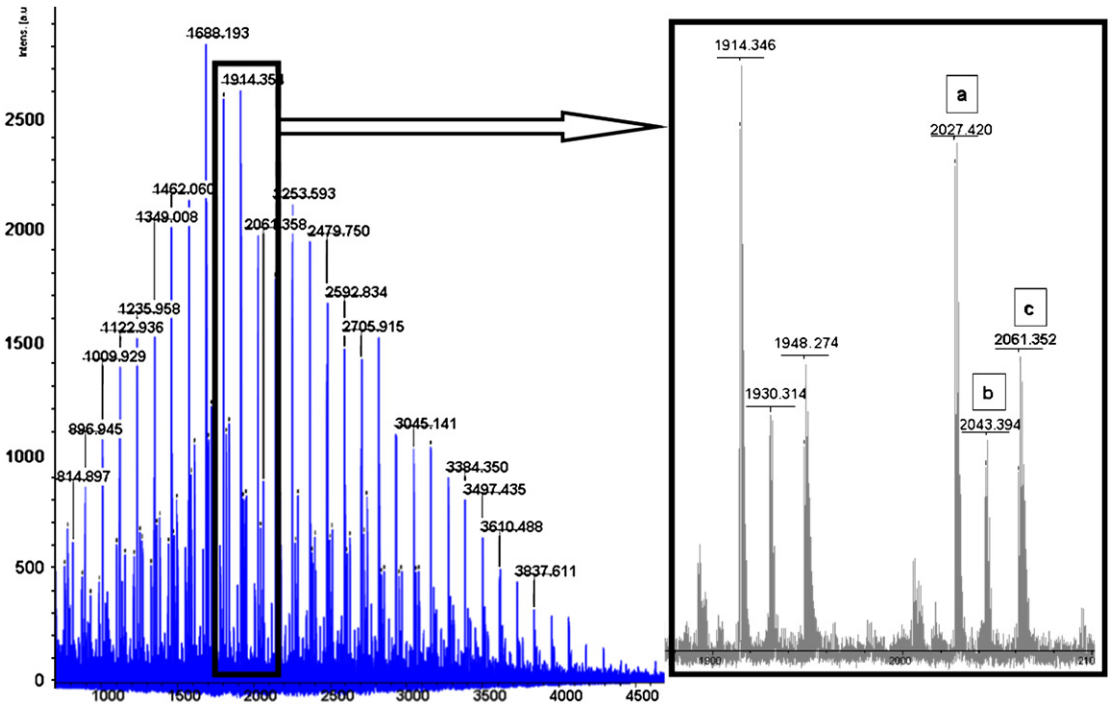

Fig. 1. MALDI-TOF spectrum of PNIPAM (sample 1, Table 1).

(10 mg/mL) in a 10:1:1 ratio. The number-average molecular weight (M_n) of polymers was determined in the linear mode.

2.8.2. Nanoparticles

Transmission electron microscopy (TEM) was carried out with a Philips CM-100 microscope. Samples were prepared by spreading a drop of a dilute dispersion of particles on a copper grid coated with Formvar. UV–vis spectra were recorded with an U3300 spectrophotometer (Hitachi). Differential scanning calorimetry (DSC) of colloidal suspension was performed under a nitrogen flow (50 cm^3/min) at a heating rate of 1 °C/min in the range of 15–60 °C with a DSC Q100 from TA Instruments.

3. Results and discussion

3.1. Synthesis and LCST of asymmetric HS–PNIPAM–COOH

α-Carboxylic acid, ω-thiol PNIPAM was synthesized as a stabilizer of gold NPs by conventional RAFT with a transfer agent of the trithiocarbonate type, i.e., 2-dodecylsulfanylthiocarbonylsulfanyl-2-methyl propionic acid (DMP). DMP was intended to cap PNIPAM by an α-carboxylic acid to be converted later on into a biotin and an ω-trithiocarbonate to be reduced into a thiol for chemisorption onto gold nanoparticles. This RAFT polymerization of NIPAM in the presence of DMP was previously reported by McCormick et al., providing PNIPAM with a controlled molecular weight and a low polydispersity [20]. Two asymmetric telechelic PNIPAMs were prepared with a number-average molecular weight (M_n, NMR) of 2500 and 4500, respectively, and a low polydispersity index (SEC) of 1.05 for both (Table 1). Although not detailed in this paper and in agreement with McCormick et al. [20], M_n linearly increased with the monomer conversion as expected for a controlled polymerization.

The PNIPAM samples were further analyzed by matrix-assisted laser desorption/ionization time-of-flight mass spectrometry (MALDI-TOF MS) in order to cross-check molecular weight and end-functionality [9a–d]. The MALDI-TOF MS spectrum showed a series of peaks (Fig. 1), with a regular interval of 113.08, which is the molar mass of the monomer. The number-average molecular weights calculated by MALDI-TOF MS (M_n, MS) were in good agreement with the NMR data (M_n, NMR) as shown in Table 1. The peaks in the MALDI-TOF MS spectrum were characteristic of PNIPAM with dodecyltrithiocarbonate and 2-methyl propionic acid as the ω- and α-end-groups, respectively. For example, the peak with a mass of 2061.35 corresponded to 15-mers of NIPAM, a DMP unit and a proton ion (c in inset of Fig. 1). No terminal unsaturation was observed, indicating that only few chains were initiated by ACPA and/or irreversibly terminated. Two other distributions were, however, observed in the spectrum that corresponded to PNIPAM without the dodecyl radical at the ω-end-group and ionized by K^+ (2043.39) (b in inset of Fig. 1) and Na^+ (2027.42) (a in inset of Fig. 1), respectively. These additional distributions more likely resulted from the cleavage of the end-group during analysis, in agreement with both Ladavière et al. in the study of poly(acrylic acid) synthesized by RAFT with a trithiocarbonic acid dibenzyl ester and Müller in the fragmentation analysis of CTA containing polymer chains [9d,e].

Several groups reported on the stabilization of gold nanoparticles by thermoresponsive polymers, including PNIPAM

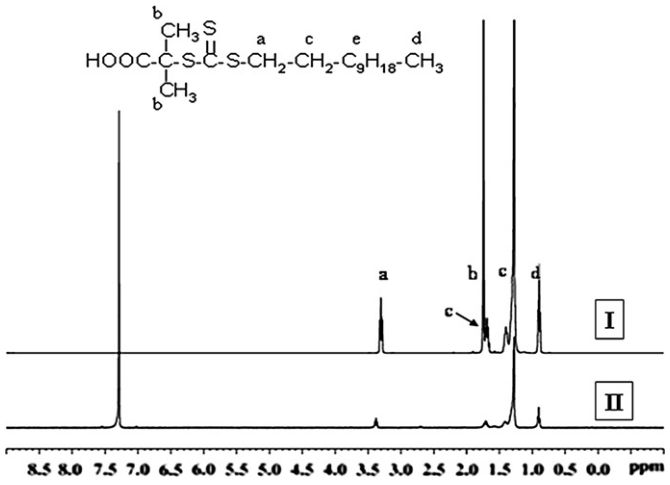

Fig. 2. ^{1}H NMR spectrum of DMP (a RAFT agent), before (I) and after (II) hydrolysis in water at pH ~ 10.

[19]. This strategy was easily implemented in the case of polymers prepared by RAFT, because the ω-dithioester or trithiocarbonate end-group was reduced into thiol simultaneously to the formation of gold nanoparticles by the Schiffrin reaction (reduction of $HAuCl_4$), thus in a one-pot process. The main drawback of using an asymmetric trithiocarbonate is the protection/stabilization of gold NPs by two types of thiol, i.e., PNIPAM–SH and alkyl–SH within a 1:1 molar ratio. As mentioned by Shan et al. [19c] differences in the gold size and the aggregation are observed when PNIPAM monolayer protected clusters are prepared directly from PNIPAMs end-capped by the asymmetric RAFT agent or from the purified hydrolyzed polymer, i.e., PNIPAM–SH and PNIPAM disulfide mixture without residual alkylthiol chains.

In this work, CTA–PNIPAM–COOH was pre-treated by NaOH in order to eliminate the alkylthiol and to form the gold NPs in the presence of the HOOC–PNIPAM–SH macroligand (Scheme 1). In this respect, Loiseau et al. reported that trithiocarbonate compounds are sensitive to hydrolysis [9e]. Therefore, the stability of DMP was tested at a pH of ~10. After 12 h, water was eliminated and the collected product was dissolved in $CDCl_3$ prior to ^{1}H NMR analysis. The solution was turbid, because of the insolubility of the cleaved HOOC–$C(CH_3)_2$–SH thiol that was removed by filtration through a 0.2 μm membrane. The peak at 1.7 ppm for the six protons adjacent to the carboxylic acid (Fig. 2I for DMP) was no longer observed for the filtrate that was consistent with dodecyl thiol released by hydrolysis of DMP (Fig. 2II).

The lower critical solution temperature (LCST) of the CTA–PNIPAM samples (Table 1) was analyzed in water by recording the increase of absorbance at 500 nm resulting from the increasing turbidity, upon raising the temperature of an aqueous solution (2 mg/mL) at a heating rate of 1.4 °C/min. A typical cloud point curve is reported in Fig. 3. The LCST was noted at the intersection of the baseline at low temperature and the tangent to the increasing absorption curve as a result of nascent turbidity.

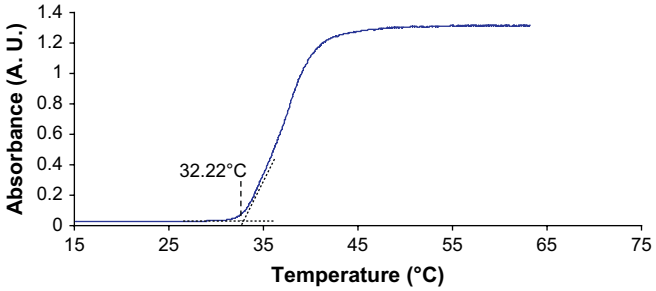

Fig. 3. Cloud point curve for PNIPAM ($M_n = 4500$) in aqueous solution (2 mg/mL) at 500 nm with a heating rate of 1.4 °C/min.

3.2. PNIPAM protected gold nanoparticles

Gold nanoparticles were prepared by the classical reduction of $HAuCl_4$ by $NaBH_4$ at 0 °C in the presence of preformed HOOC–PNIPAM–SH ($M_n = 2500$ and 4500) (Scheme 1).

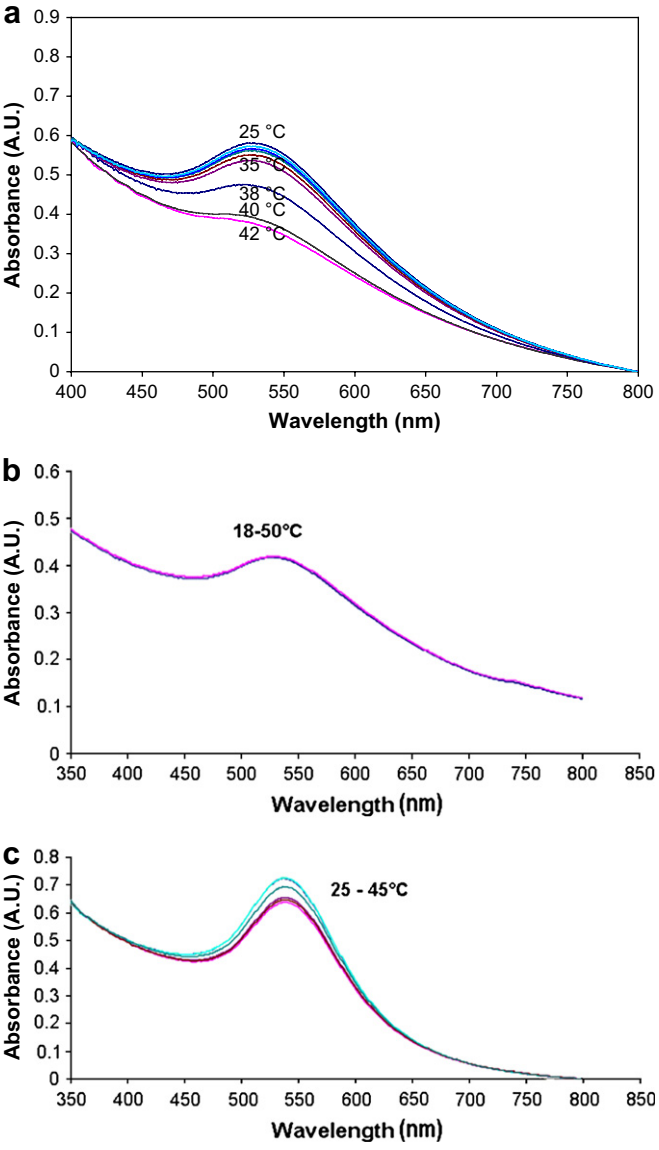

Fig. 4. Surface plasmon resonance of gold nanoparticles stabilized by PNIPAM at different temperatures: (a) Au–S–PNIPAM (4500), (b) Au–S–PNIPAM (2500) and (c) Au–PNIPAM (no thiol involved).

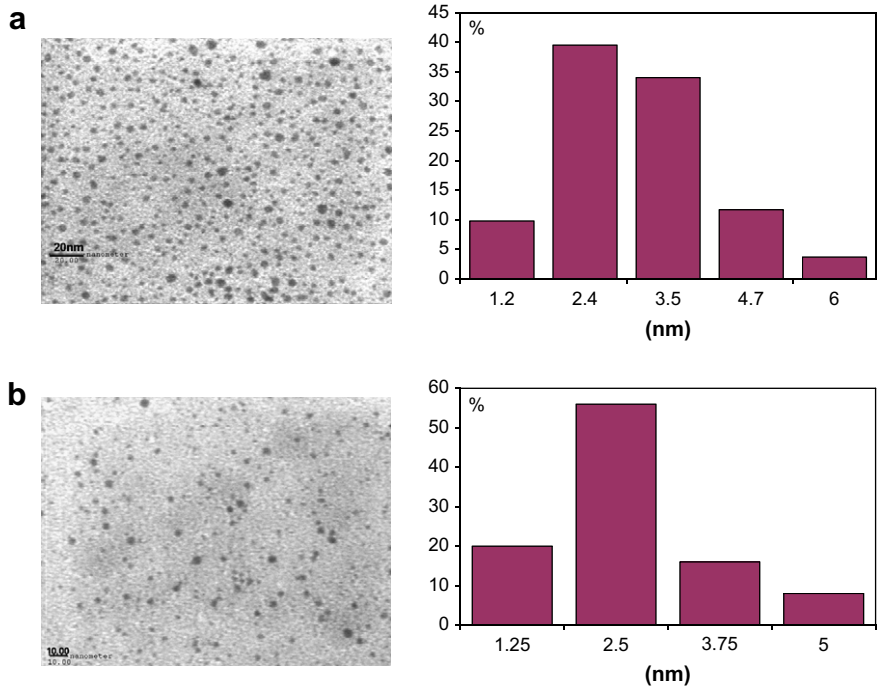

Fig. 5. TEM images of gold nanoparticles stabilized by (a) PNIPAM ($M_n = 4500$) prepared by RAFT and (b) PNIPAM prepared by free-radical polymerization (no thiol involved).

The colloidal suspensions were very stable and characterized by absorption at 530 nm (Fig. 4). The protected/stabilized gold nanoparticles were observed by TEM with an average size of 2.5 ± 0.5 nm and a narrow size distribution for the two suspensions (Fig. 5). Surprisingly enough, gold nanoparticles stabilized by HOOC–PNIPAM–SH of the lower molecular weight did not show any temperature response even until 50 °C (Fig. 6, sample a). In sharp contrast, those ones stabilized by HOOC–PNIPAM–SH of the higher molecular weight were remarkably temperature-sensitive (Fig. 6, sample b). The characteristic absorbance of the aqueous solution of the PNIPAM stabilized gold nanoparticles was recorded throughout the LCST temperature range of the non-adsorbed chains. For the temperature dependence of the surface plasmon to be observed properly, the effect of the solution turbidity was taken into account by subtracting the absorbance increment at 400 nm and normalizing the curves such that the absorbance ranged from 0 to 0.9 [24]. The absorbance typically decreased with increasing temperature for the solution of NPs stabilized by HOOC–PNIPAM–SH (4500) (Fig. 4a)

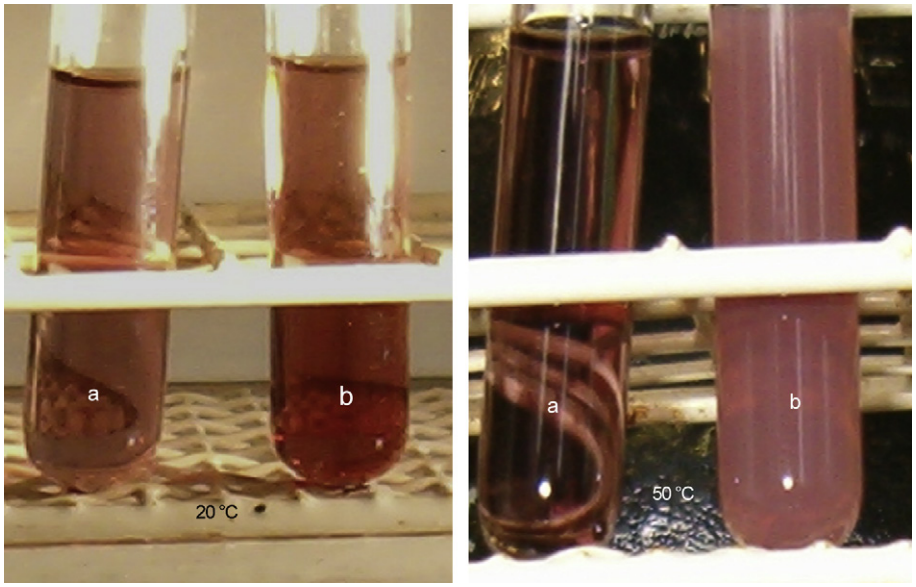

Fig. 6. Gold nanoparticles stabilized by (a) PNIPAM–SH ($M_n = 2500$) and (b) PNIPAM–SH ($M_n = 4500$) at 20 and 50 °C, respectively.

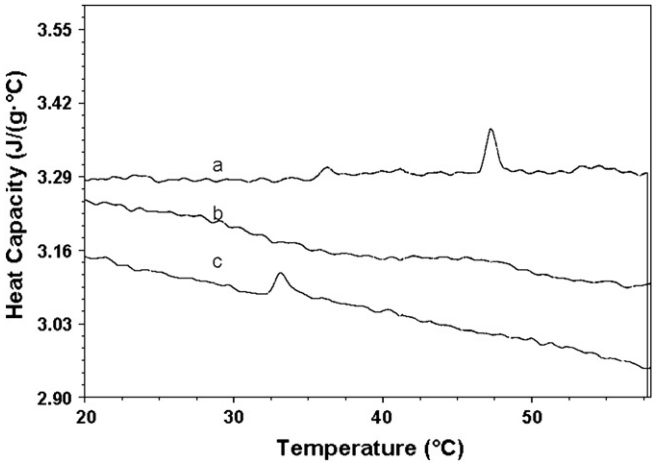

Fig. 7. Microcalorimetric endotherms for aqueous dispersions of (a) RAFT-PNIPAM (Table 1, entry 2), (b) RAFT-PNIPAM (entry 1) and (c) PNIPAM (entry 3).

as result of the shielding of the gold surface by collapsed PNIPAM chains. At 25 °C, the characteristic plasmon resonance at 530 nm was clearly detected, which was not the case anymore above 35 °C. The surface plasmon resonance is known to depend on several parameters, such as the refractive index of both the solvent and the protective shell layer [24]. A discontinuity in the absorbance at 530 nm was observed in the LCST domain (Fig. 4a), which is the signature of the dehydration of PNIPAM and the related modification of the refractive index [19a]. Consistent with the temperature insensitivity of the gold nanoparticles stabilized by HOOC–PNIPAM–SH of $M_n = 2500$, the plasmon resonance did not change from 18 to 50 °C (thus through the LCST range of the original macroligand; Fig. 4b).

For the sake of comparison, gold nanoparticles were prepared in the presence of PNIPAM, synthesized by free-radical polymerization, thus deprived of any thiol end-group. The apparent molecular weight (M_n, SEC) was approximately two times higher than that one of HOOC–PNIPAM–SH with a nominal M_n (M_n, NMR) of 4500 (Table 1). The polydispersity was also much high ($M_w/M_n = 2$). Formation of gold nanoparticles of the same average size as before (2.5 ± 0.5 nm) and a narrow size distribution was observed by TEM (Fig. 5b). Consistently, the UV–vis spectrum showed absorption at 536 nm, characteristic of the surface plasmon resonance of well-spaced gold NPs (Fig. 4c). Clearly, PNIPAM, with or without a thiol end-group, has the ability to passivate a gold surface. According to Remacle et al., the constitutive amides of PNIPAM can interact with gold via N–H···Au hydrogen bonds and still stronger Au–O bonds [25]. As an additional piece of information, the microcalorimetric endotherms of the aqueous suspension of gold nanoparticles stabilized by the different PNIPAM chains were recorded (Fig. 7). As far as NPs stabilized by RAFT-PNIPAM (Table 1, entry 2) are concerned, two separate transition processes at $T_{m1} = 37 \pm 0.6$ °C and $T_{m2} = 48 \pm 0.7$ °C are observed (Fig. 7, graph a) as already reported by Shan et al. [19c]. Both transitions are 5 °C higher than those reported by Shan for 4-cyanopentanoic acid PNIPAM ($M_n = 5400$) stabilized gold NPs [19e]. This difference can be understood by

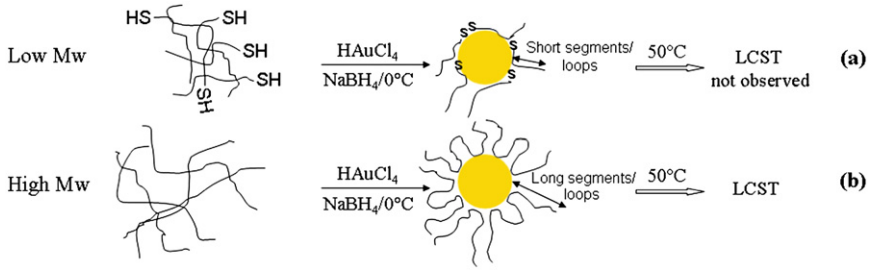

Scheme 2. Train-loop-tail model for the adsorption of PNIPAM onto the gold surface.

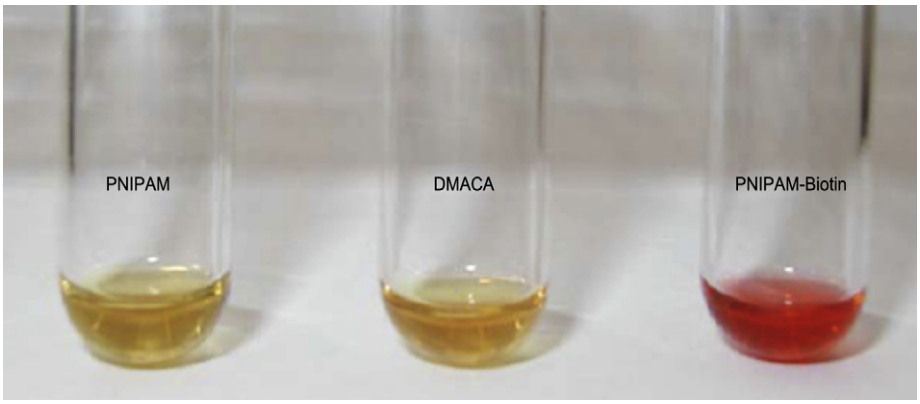

Fig. 8. Colorimetry of biotinylated PNIPAM by DMACA.

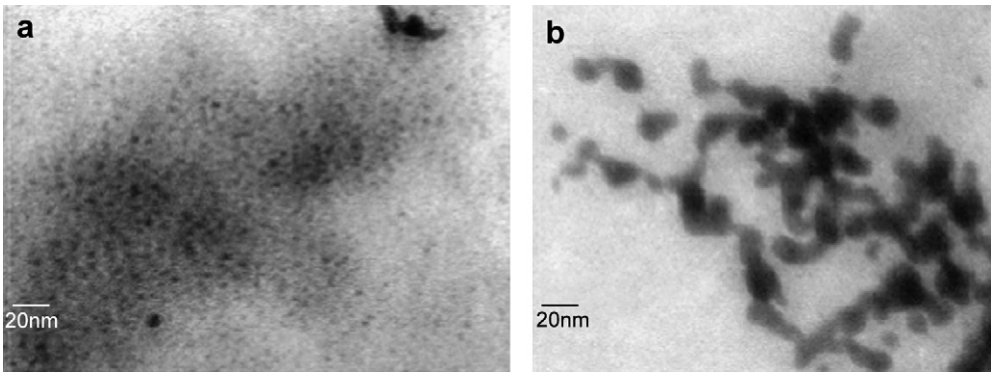

Fig. 9. TEM images of gold nanoparticles (a) stabilized by Bio-PNIPAM-SH and (b) idem after supramolecular assembly by complexation with avidin.

different end-groups for PNIPAM chains in addition to slightly different working conditions (heating rate 1 °C/min in the present case). The occurrence of two endotherms has been previously explained by difference in the hydratation degree of the PNIPAM brush considering two zones around the gold nanoparticles. The poorly hydrated chains of the inner zone collapse at lower temperature than that of the hydrated outer zone.

In the case of PNIPAM (Table 1, entry 3) coated gold, only one broad endotherm centered at 33 ± 0.8 °C was observed (Fig. 7, graph c). This is in line with the replacement of the brush-like morphology [19e] expected for "RAFT-PNIPAM" (Table 1, entry 2) by the random train-loop-tail adsorption of PNIPAM (entry 3) [19f]. The broadening of this endotherm may be due to the heterogeneity of the molar mass of the hydrated PNIPAM segments caused by the random interaction of amid functions with gold surface. Finally, as expected for PNIPAM obtained by RAFT (Table 1, entry 1), no significant endotherm was observed (Fig. 7, graph b), due to the poor hydratation of the low molecular weight PNIPAM brush in line with the collected UV data.

Based on the Tenhu et al. [19e] explanation of these observations, i.e., a first transition characteristic of the PNIPAM segments close to the gold surface, thus densely packed and less hydrated, whereas the fully hydrated segments located away from the surface would be responsible for the second transition and on the well-known dependence of LCST on the PNIPAM molecular weight, we propose the following model for the PNIPAM chains at the gold surface (Scheme 2). Independently of the thiol end-group, which is chemisorbed to the surface, the random adsorption of constitutive amide units results in dangling loops and terminal segments, whose relative length allows the LCST to manifest itself or not. This model actually fits the train-loop-tail conformation proposed for poly(ethylene oxide) (PEO) [26] and poly(vinyl pyrrolidone) (PVP) [27] adsorbed onto silica. Finally, biotin was attached to the protective shell of the gold nanoparticles by amidification of the carboxylic acid end-groups of the PNIPAM stabilizer.

Thus the acid function of HS–PNIPAM–COOH was activated by *N*-hydroxysuccinimide and then reacted with *N*-(5-aminopentyl)biotinamide in the presence of triethylamine. Biotinylated PNIPAM was purified by dialysis and recovered by lyophilization. Qualitatively the success of biotinylation was confirmed by a coloration test [28]. Indeed, the yellow color of 7-dimethylaminocoumarin-4-acetic acid (DMACA) turned pink in the presence of PNIPAM–biotin (Fig. 8; for interpretation of the references to color in this figure, the reader is referred to the web version of this article). Biotinylated PNIPAM was used as a stabilizer in the preparation of gold nanoparticles according to the same recipe as before. Gold nanoparticles stabilized by Bio-PNIPAM–SH were observed by TEM. Fig. 9a shows particles with a size in the 1–5 nm range. Upon addition of avidin, the suspension of gold nanoparticles stabilized by biotinylated PNIPAM became turbid (Fig. 10) consistent with the observation of strings of nanoparticles by TEM (Fig. 9b). These preliminary observations are promising for converting the PNIPAM coated gold NPs into building blocks of supramolecular assemblies. As a rule, complexation of biotinylated PNIPAM with (strept)avidin is an expected versatile tool to confer thermosensitivity to avidin containing molecules (e.g., drugs and antibodies), surfaces and particles with potential application in drug delivery, biotechnology and surface engineering.

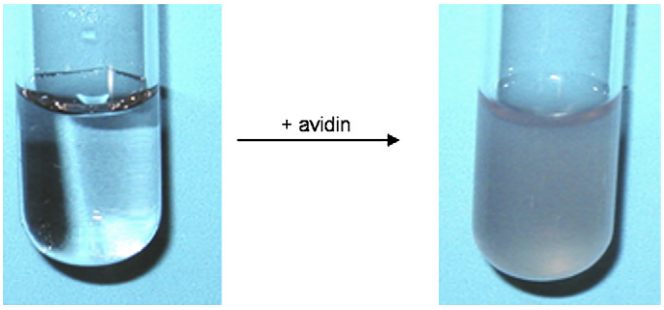

Fig. 10. Gold nanoparticles stabilized by biotinylated PNIPAM before and after addition of avidin.

4. Conclusions

Gold nanoparticles were prepared by reduction of $HAuCl_4$ in the presence of thermosensitive PNIPAM. Although thiol end-capped PNIPAM is known as a macroligand effective in stabilizing gold nanoparticles, this work showed that interactions between constitutive amides of PNIPAM and gold are strong enough to protect gold nanoparticles against

aggregation. A train-loop-tail model, as was reported for the adsorption of PEO and PVP on silica, would also prevail at the PNIPAM/gold interface. It is only when the length of the dangling PNIPAM segments is long enough that the LCST behavior of the polymer can manifest itself. α-Carboxylic acid, ω-thiol PNIPAM was synthesized by RAFT, and the acid end-group was used to attach biotin in the α-position. Gold nanoparticles stabilized by biotinylated PNIPAM are prone to organization at the supramolecular level by biotin/avidin complexation.

Acknowledgments

The authors are grateful to 'Région Wallonne' for support in the frame of the ''NOMADE'' programme. A.A. and C.J. are also indebted to ''Belgian Science Policy'' for financial support in the frame of the ''Interuniversity Attraction Poles Programme (PAI 6/27) – Functional Supramolecular Systems''. C.J. is a Research Associate of the ''Fonds National de la Recherche Scientifique (FNRS)''.

References

[1] Kenneth J, Klabunde, editors. Nanoscale materials in chemistry. Wiley-Interscience; September 14, 2001.
[2] Vossmeyer T, Guse B, Besnard I, Bauer RE, Muller K, Yasuda A. Adv Mater 2002;14:238–42.
[3] Storhoff JJ, Elghanian R, Mucic RC, Mirkin CA, Letsinger RL. J Am Chem Soc 1998;120:1959–64.
[4] Maier SA, Brongersma ML, Kik PG, Meltzer S, Requicha AAG, Atwater HA. Adv Mater 2001;13:1501–5.
[5] (a) Longo A, Calandra P, Casaletto MP, Giordano C, Venezia AM, Liveri VT. Mater Chem Phys 2006;96(1):66–72;
(b) Qiu H, Rieger J, Gilbert B, Jérôme R, Jérôme C. Chem Mater 2004;16(5):850–6.
[6] Aqil A, Detrembleur C, Gilbert B, Jerome R, Jerome C. Chem Mater 2007;19:2150–4.
[7] Corbierre MK, Cameron NS, Lennox RB. Langmuir 2004;20(7):2867–73.
[8] Yim H, Kent MS. Macromolecules 2004;37:1994–7.
[9] (a) Ganachaud F, Monteiro MJ, Gilbert RG, Dourges MA, Thang SH, Rizzardo E. Macromolecules 2000;33:6738–45;
(b) Masci G, Giacomelli L, Crescenzi V. Macromol Rapid Commun 2004;25:559–64;
(c) Xia Y, Yin X, Burke NAD, Stöver HDH. Macromolecules 2005; 38:5937–43;
(d) Schilli CM, Lanzendörfer MG, Müller AHE. Macromolecules 2002; 35:6819–27;
(e) Loiseau J, Doërr N, Suau JM, Egraz JB, Llauro MF, Ladavière C. Macromolecules 2003;36:3066–77.
[10] Sun T, Wang G, Feng L, Liu B, Ma Y, Jiang L, et al. Angew Chem Int Ed 2004;43:357–60.
[11] Hoffman AS. J Controlled Release 1987;6:297.
[12] Stayton PS, Shimoboji T, Long C, Chilkoti A, Chen G, Harris JM, et al. Nature (London) 1995:378–472.
[13] Park YS, Ito Y, Imanishi Y. Langmuir 1998;14:910.
[14] Bergbreiter DE, Osburn PL, Wilson A, Sink EM. J Am Chem Soc 2000;122:9085.
[15] (a) Pelton RH, Chibante P. Colloids Surf 1986;20:247;
(b) Pelton RH. Adv Colloid Interface Sci 2000;85:1.
[16] Kizhakkedathu JN, Jones RN, Brooks DE. Macromolecules 2004; 37:734–43.
[17] Tsarevsky NV, Matyjaszewski K. Polym Prepr 2002;43(2):205.
[18] (a) Ray B, Isobe Y, Morioka K, Habaue S, Okamoto Y, Kamigaito M, et al. Macromolecules 2003;36:543–5;
(b) Baussard JF, Habib-Jiwan JL, Laschewsky A, Mertoglu M, Storsberg J. Polymer 2004;45:3615–26;
(c) Wan D, Pu H. Mater Lett 2007;61:3404–8.
[19] (a) Raula J, Shan J, Nuopponen M, Niskanen A, Jiang H, Kauppinen EI, et al. Langmuir 2003;19:3499–504;
(b) Zhu MQ, Wang LQ, Exarhos GJ, Li ADQ. J Am Chem Soc 2004; 126:2656–7;
(c) Shan J, Nuopponen M, Jiang H, Tenhu H. Macromolecules 2003; 36:4526–33;
(d) Sumerlin BS, Donovan MS, Mitsukami Y, Lowe AB, McCormick CL. Polym Prepr 2002;43(2):313;
(e) Shan J, Nuopponen M, Jiang H, Viitala T, Kauppinen E, Kontturi K, et al. Macromolecules 2005;38:2918–26;
(f) Shan J, Chen J, Nuopponen M, Tenhu H. Langmuir 2004;20:4671–6.
[20] Convertine AJ, Ayres N, Scales CW, Lowe AB, McCormick CL. Biomacromolecules 2004;5:1177–80.
[21] Lai JT, Filla D, Shea R. Macromolecules 2002;35:6754–6.
[22] Lowe AB, Sumerlin BS, Donovan MS, McCormick CL. J Am Chem Soc 2002;124:11562–3.
[23] Leff DV, Ohara PC, Heath JR, Gelbart WM. J Phys Chem 1995;99: 7036.
[24] Shan J, Chen J, Nuopponen M, Viitala T, Jiang H, Peltonen J, et al. Langmuir 2006;22:794–801.
[25] (a) Kryachko ES, Remacle F. J Phys Chem B 2005;109(48):22746–57;
(b) Kryachko ES, Remacle F. Chem Phys Lett 2005;404(1–3):142–9;
(c) Kryachko ES, Remacle F. Nano Lett 2005;5(4):735–9.
[26] Maltesh C, Somasundaran P, Ramachandran R. J Appl Polym Sci 1990;45(2):329–38.
[27] Thibaut A, Misselyn-Bauduin AM, Broze G, Jerome R. Langmuir 2000; 16(25):9841–9.
[28] Vanwetswinkel S, Touillaux R, Fastrez J, Brynaert JM. Bioorg Med Chem 1995;3(7):907–15.